This article was downloaded by:
On: *25 January 2011*
Access details: *Access Details: Free Access*
Publisher *Taylor & Francis*
Informa Ltd Registered in England and Wales Registered Number: 1072954 Registered office: Mortimer House, 37-41 Mortimer Street, London W1T 3JH, UK

Separation Science and Technology
Publication details, including instructions for authors and subscription information:
http://www.informaworld.com/smpp/title~content=t713708471

A Predictive Model for Permeation Flux in a Membrane Reactor: Aspects of Esterification

Henry Kasaini[a]; Lorraine Malherbe[a]; Raymond Everson[a]; Klaas Keizer[a]; Hein Neomagus[a]
[a] School of Chemical and Minerals Engineering, Separation Science and Technology Group, North-West University, Potchefstroom, South Africa

To cite this Article Kasaini, Henry , Malherbe, Lorraine , Everson, Raymond , Keizer, Klaas and Neomagus, Hein(2005) 'A Predictive Model for Permeation Flux in a Membrane Reactor: Aspects of Esterification', Separation Science and Technology, 40: 1, 433 — 452
To link to this Article: DOI: 10.1081/SS-200042490
URL: http://dx.doi.org/10.1081/SS-200042490

PLEASE SCROLL DOWN FOR ARTICLE

Full terms and conditions of use: http://www.informaworld.com/terms-and-conditions-of-access.pdf

This article may be used for research, teaching and private study purposes. Any substantial or systematic reproduction, re-distribution, re-selling, loan or sub-licensing, systematic supply or distribution in any form to anyone is expressly forbidden.

The publisher does not give any warranty express or implied or make any representation that the contents will be complete or accurate or up to date. The accuracy of any instructions, formulae and drug doses should be independently verified with primary sources. The publisher shall not be liable for any loss, actions, claims, proceedings, demand or costs or damages whatsoever or howsoever caused arising directly or indirectly in connection with or arising out of the use of this material.

Separation Science and Technology, 40: 433–452, 2005
ISSN 0149-6395 print/1520-5754 online
DOI: 10.1081/SS-200042490

A Predictive Model for Permeation Flux in a Membrane Reactor: Aspects of Esterification

Henry Kasaini, Lorraine Malherbe, Raymond Everson, Klaas Keizer, and Hein Neomagus
School of Chemical and Minerals Engineering, Separation Science and Technology Group, North-West University, Potchefstroom, South Africa

Downloaded At: 09:58 25 January 2011

Abstract: A polymeric membrane (PERVAP® 2201) was used to study permselectivity and flux of water from esterification mixtures at different temperatures (30°C–90°C) and compositions. The pervaporation flux of water from binary mixtures such as butyl acetate/H_2O, butanol/H_2O, and acetic acid/H_2O was accurately predicted by using a solution-diffusion model with concentration-dependent diffusion coefficients. Furthermore, on the basis of a lower activation energy of diffusion and higher flux for water, we concluded that butyl acetate production can be enhanced significantly by inserting a reactor membrane (PERVAP® 2201)in the esterification process.

INTRODUCTION

Esterification of glycol ethers or aliphatic alcohols with acetic acid is a well-known and important industrial process. The esterification reaction that occurs when butyl acetate is produced in the presence of an acid catalyst (1) is shown below.

This research study was funded by the Sasol Centre of Separation and Technology (SST), and South Africa National Research Foundation (NRF).

Address correspondence to Henry Kasaini, School of Chemical and Minerals Engineering, Separation Science and Technology Group, North-West University, Potchefstroom Campus, Private Bag X6001, Potchefstroom 2520, South Africa. Tel.: + 27 18 299-1664; Fax: ++ 27 18 299-1535; E-mail: chihk@puknet.puk.ac.za

The esterification reaction is reversible, and usually an equilibrium is established where the stoichiometric ratio of alcohol to the ester reaches a constant value. To achieve a higher ester yield, it is customary to drive the equilibrium position to the right side by either using a large excess of one of the reactants or using a reactive distillation process to accomplish in situ removal of product(s) (2). A reactive distillation process is only effective when the difference between the volatility of the product and reactant species is sufficiently large. If the esterification mixture forms an azeotrope, a simple reactive distillation process would be inadequate to produce the required result. Several researchers have therefore suggested that acetate production could be enhanced when a separation unit is coupled to an esterification process (3–6). For example, the selective removal of water molecules by membrane reactors impacts positively on the conversion of reactants (butanol and acetic acid) to the acetate product.

Downloaded At: 09:58 25 January 2011

Theory of Sorption

Preferential sorption of a component occurs if the composition of the binary mixture inside the polymer is different from the composition of the feed mixture. The relative volume fraction of component i from a binary mixture into the membrane phase, u_i, is defined in Eq. (1):

$$u_i = \frac{\phi_i}{\phi_1 + \phi_2} = \frac{\phi_i}{1 - \phi_3}, \ldots i = 1, 2 \tag{1}$$

where ϕ_i is the volume fraction of component i in the ternary (membrane) phase. If the concentration in the liquid phase is given by v_i, then the preferential sorption, ε, specific to the membrane is expressed as

$$\varepsilon = u_1 - v_1 = v_2 - u_2 \tag{2}$$

The condition for equilibrium between the binary feed phase and the ternary polymer phase is expressed by the equality of the chemical potentials, μ_i, in the two phases. Intermolecular interactions are, however, large in the liquid state owing to the closeness of the molecules. Flory (7) suggested that since the pure liquids and the polymer are taken as reference states for the treatment of the solution, it is only the difference between the total interaction energy in the solution as compared with that for the pure liquid components that is important. At equilibrium, the chemical potentials in terms of osmotic pressure, Π, are shown by Eqs. (3) and (4):

$$\Delta\mu_1^o = \Delta\mu_1^m + \Pi V_1 \tag{3}$$

$$\Delta\mu_2^o = \Delta\mu_2^m + \Pi V_2 \tag{4}$$

where the polymer-free phase is denoted by the superscript o and the ternary phase with the superscript m. V_i is the molar volume of component i.

Various thermodynamic theories have been proposed and applied to interpret sorption equilibria in polymeric membranes of which the Flory-Huggins theory and its extensions are the most widely used (8). Therefore, chemical potentials of the equilibrium system described in Eqs. (3) and (4) can be obtained from Flory-Huggins thermodynamics. The Gibbs free energy of mixing, ΔG_M, can be expressed as follows:

$$\Delta G_M = \Delta H_M - T\Delta S_M \tag{5}$$

where ΔH_M and ΔS_M are the enthalpy and entropy changes on mixing, respectively. For real solutions, ΔH_M and ΔS_M can be expressed as

$$\Delta H_M = RT \sum_{i<j} n_i \phi_i g_{ij} \tag{6}$$

$$\Delta S_M = -R \sum n_i \ln \phi_i \tag{7}$$

where R is the universal gas constant, n_i the mole fraction of component i in the ternary phase, and g_{ij} the concentration dependent binary interaction parameter. For a three-component system, substitution of Eqs. (6) and (7) into Eq. (5) reduces to Eq. (8) (9, 10).

$$\begin{aligned}\frac{\Delta G_M}{RT} = {} & n_1 \ln \phi_1 + n_2 \ln \phi_2 + n_3 \ln \phi_3 + g_{12}(u_2) n_1 \phi_2 \\ & + g_{13}(u_2, \phi_3) n_1 \phi_3 + g_{23}(u_1, \phi_3) n_2 \phi_3\end{aligned} \tag{8}$$

The binary interaction parameters, g_{12}, g_{13}, and g_{23}, are assumed to be concentration-dependent. For the liquid mixture in the polymer, g_{12} is assumed to be independent of the polymer concentration and is thus only a function of $u_2(g_{12}(u_2))$. The g_{13} and g_{23} parameters are assumed to be functions of $u_i (i = 1,2)$ and ϕ_3 ($g_{13}(u_2, \phi_3)$, and $g_{23}(u_1, \phi_3)$). In the original Flory-Huggins theory the interaction parameters that they used were concentration-independent (11).

The chemical potential, μ_i, of a component in a solution relative to its chemical potential in the pure liquid, μ_i^o, is obtained by differentiating the free energy of mixing with respect to the mole fraction, n_i, in the ternary phase. Thus, differentiation of Eq. (8) with respect to n_1 and n_2, respectively,

Downloaded At: 09:58 25 January 2011

yields Eqs. (9) and (10) for the chemical potentials of the different components in the polymer phase, μ_i^m.

$$\begin{aligned}\frac{\Delta\mu_1^m}{RT} &= \ln\phi_1 + \phi_2\left(1-\frac{V_1}{V_2}\right) + \phi_3\left(1-\frac{V_1}{V_3}\right)\\ &\quad + (g_{12}\phi_2 + g_{13}\phi_3)(\phi_2+\phi_3)\\ &\quad - u_1u_2\phi_2\frac{\partial g_{12}}{\partial u_2} - g_{23}\frac{V_1}{V_2}\phi_2\phi_3 - u_1u_2\phi_3\frac{\partial g_{13}}{\partial u_2} - \phi_1\phi_3^2\frac{\partial g_{13}}{\partial\phi_3}\\ &\quad + \frac{V_1}{V_2}u_2^2\phi_3\frac{\partial g_{23}}{\partial u_1} - \frac{V_1}{V_2}\phi_2\phi_3^2\frac{\partial g_{23}}{\partial\phi_3}\end{aligned} \tag{9}$$

$$\begin{aligned}\frac{\Delta\mu_2^m}{RT} &= \ln\phi_2 + \phi_1\left(1-\frac{V_2}{V_1}\right) + \phi_3\left(1-\frac{V_2}{V_3}\right)\\ &\quad + \left(g_{12}\frac{V_2}{V_1}\phi_1 + g_{23}\phi_3\right)(\phi_1+\phi_3)\\ &\quad - \frac{V_2}{V_1}u_1^2\phi_2\frac{\partial g_{12}}{\partial u_2} - g_{13}\frac{V_2}{V_1}\phi_1\phi_3 + \frac{V_2}{V_1}u_1^2\phi_3\frac{\partial g_{13}}{\partial u_2}\\ &\quad - \frac{V_2}{V_1}\phi_1\phi_3^2\frac{\partial g_{13}}{\partial\phi_3} - u_1u_2\phi_3\frac{\partial g_{23}}{\partial u_1} - \phi_2\phi_3^2\frac{\partial g_{23}}{\partial\phi_3}\end{aligned} \tag{10}$$

The Gibbs free energy of mixing for the binary phase is expressed as (9, 10)

$$\frac{\Delta G_M}{RT} = x_1\ln v_1 + x_2\ln v_2 + g_{12}(v_2)x_1v_2 \tag{11}$$

Differentiation of Eq. (11) with respect to x_1 and x_2 yields

$$\frac{\Delta\mu_1^o}{RT} = \ln v_1 + \left(1-\frac{V_1}{V_2}\right)v_2 + g_{12}v_2^2 - v_1v_2^2\frac{\partial g_{12}}{\partial v_2} \tag{12}$$

$$\frac{\Delta\mu_2^o}{RT} = \ln v_2 + \left(1-\frac{V2}{V_1}\right)v_1 + \frac{V_2}{V_1}g_{12}v_1^2 + \frac{V_2}{V_1}v_2v_1^2\frac{\partial g_{12}}{\partial v_2} \tag{13}$$

If it is assumed that $V_1/V_3 \cong V_2/V_3 \cong 0$ (i.e., the molar volume of the membrane = the molar volume of the components in the feed mixture) and that $V_1/V_2 = r$, then substitution of Eqs. (9), (10), (12), and (13) in Eqs. (3) and (4) and elimination of the osmotic pressure, Π, leads to Eq. (14):

$$\begin{aligned}\ln\left(\frac{\phi_1}{\phi_2}\right) - \ln\left(\frac{v_1}{v_2}\right) &= (r-1)\ln\left(\frac{\phi_2}{v_2}\right) - g_{12}(u_2)\left(\phi_2-\phi_1\right)\\ &\quad - g_{12}(v_2)(v_1-v_2) - \phi_3(g_{13}-rg_{23}) + u_1\phi_2\frac{\partial g_{12}}{\partial u_2}\\ &\quad - v_1v_2\frac{\partial g_{12}}{\partial v_2} + \phi_3u_1\frac{\partial g_{13}}{\partial u_2} - \frac{V_1}{V_2}u_2\phi_3\frac{\partial g_{23}}{\partial u_1}\end{aligned} \tag{14}$$

Downloaded At: 09:58 25 January 2011

At a given volume fraction of penetrant in the feed, v_i, the theoretical values of the preferential sorption can thus be calculated from Eq. (14) if the interaction parameters, the ratio of the molar volumes, r, and the volume fraction of the polymer, ϕ_3 (or the overall sorption), are known. Therefore, it follows that the preferential sorption depends on the difference in molar volumes of the two penetrants, the affinity of both components toward the polymer, and the mutual interaction between the two penetrants.

Evaluation of Interaction Parameters

There are two methods that could be used to determine the interaction parameters of a polymer and a nonsolvent: equilibrium-swelling experiments and inverse-gas chromatography. The disadvantage of the latter method is that interaction parameters are obtained for infinite polymer concentrations, χ^{∞}, at elevated temperatures. Because the interaction parameter is usually temperature- and concentration-dependent, extrapolation is difficult. However, swelling experiments are comparatively easier to perform at various temperatures. The membrane can be considered as a swollen gel or a network with cross-links caused by crystalline regions, chain entanglements, or Van der Waals interactions. The swelling behavior of such a network can be expressed by the Flory-Rehner theory (11). The free-energy change, ΔG, involved in the mixing of the pure solvent with the initially pure polymer consists of two parts: the free energy of mixing, ΔG_M, and the elastic free energy, ΔG_{el}.

$$\Delta G = \Delta G_M + \Delta G_{el} \tag{15}$$

At swelling equilibrium, $\Delta G = 0$, and the Flory-Rehner theory postulates that

$$\ln(1 - \phi_3) + \phi_3 + \chi\phi_3^2 + \frac{V_1}{M_c\phi_3}\left(\phi_3^{1/3} - 0.5\phi_3\right) = 0 \tag{16}$$

In polymer-nonsolvent systems with small amounts of nonsolvent in the polymer, the last term in Eq. (16) can be neglected to obtain Eq. (17), which is the interaction parameter of a single component with the membrane, thus

$$\chi_{i3} = -\frac{[\ln(1 - \phi_3) + \phi_3]}{\phi_3^2} \tag{17}$$

Concentration-Dependent Binary Interaction Parameters g_{13} and g_{23}

The binary interaction parameters are considered to be concentration dependent when ternary effects are taken into account. Mulder et al. (12)

Downloaded At: 09:58 25 January 2011

proposed mathematical expressions for these parameters as

$$g_{13} = \chi_{13} + au_2 + b[\phi_3 - \phi_3(u_2 \to 0)] \tag{18}$$

$$g_{23} = \chi_{23} + cu_1 + d[\phi_3 - \phi_3(u_1 \to 0)] \tag{19}$$

where a, b, c, and d are constants. For the limiting cases when $u_2 \to 0$ and $u_1 \to 0$, Eqs. (18) and (19) reduce to χ_{13} and χ_{23}.

The concentration-dependent binary interaction parameter, g_{12}, can be determined from the Flory-Huggins thermodynamics. Flory et al. (11) and Yang et al. (13) showed that for a binary system the activity, a_1, is expressed as

$$\ln a_1 = \ln v_1 + \left(1 - \frac{V_1}{V_2}\right)v_2 + g_{12}v_2^2 \tag{20}$$

The activity, a_1, can be computed by using ASPEN Tech V10 with the relevant thermodynamic model. Subsequently, the dependence of g_{12} on v_2 can be expressed as a relation, and the value of g_{12} can then be calculated at any given value of v_2.

Downloaded At: 09:58 25 January 2011

Theory of Permeation Flux

According to the solution-diffusion model (14), the flux of component i through the membrane is proportional to the chemical potential gradient across the membrane

$$J_i = -C_i B_i \frac{d\mu_i}{dl} \tag{21}$$

where C_i is the concentration of component I, and B_i is the mobility in the membrane. If the chemical potential at constant temperature is related to the species activity then

$$J_i = -C_i D_i \frac{d \ln a_i}{dl} \tag{22}$$

where

$$D_i = RTB_i \tag{23}$$

Equation (22) can be expanded to incorporate different expressions for solubilities and diffusivities, thus permeation flux is obtained.

$$J_i = \frac{\rho_i}{L}\int_0^{\phi_{i0}} D_i d\phi_i = \frac{\rho_i}{L}\int_0^{\phi_{i0}} (D_T)_i \frac{\partial \ln a_i}{\partial \ln \phi_i} d\phi_i \tag{24}$$

where the concentration-dependent diffusion coefficients are expressed as

$$(D_T)_1 = D_{0,1} \exp\left(\frac{-E_{D,1}}{RT}\right)(1 + \kappa_{11}\phi_1 + \lambda_{12}\phi_2) \tag{25}$$

$$(D_T)_2 = D_{0,2} \exp\left(\frac{-E_{D,2}}{RT}\right)(1 + \kappa_{21}\phi_1 + \lambda_{22}\phi_2) \tag{26}$$

and κ_{ij} and λ_{ij} are constants, and $D_{0,\mathrm{i}}$ is the diffusion coefficient at infinite dilution. Parameters $D_{0,\mathrm{i}}$, $E_{D,\mathrm{i}}$, κ_{ij}, and λ_{ij} can be assumed by referring to previously published data and then regressed.

EXPERIMENTAL

The membrane that we used in this study is an asymmetric and composite polymeric membrane (PERVAP® 2201), which was supplied by Sulzer Chemtech Co., South Africa. The membrane has a thin dense layer (2–4-μm thick) of cross-linked PVA supported on a microporous substrate (woven substructure). The thin surface layer is nonporous and serves as the separation medium. But, the porous substructure provides mechanical strength.

Downloaded At: 09:58 25 January 2011

Swelling and Sorption Tests

Swelling experiments were performed to measure the optimum uptake of liquid by the membrane and to determine the composition of encapsulated liquid mixtures. The experimental method that we applied has been reported in the literature (14, 15). The mass percentage uptake of liquid, M_t, of the polymer samples by the solvent molecules was calculated using Eq. (27)

$$M_t = \left[\frac{W_t - W_o}{Wo}\right] \times 100 \tag{27}$$

where W_t and W_o are the membrane masses after and before solvent uptake, respectively. The composition of the liquid mixture inside the membrane was determined by using the apparatus given in Fig. 1, which was also applied by Yoshikawa et al. (16). After sorption had reached an equilibrium, the membrane sample, loaded with the solution, was inserted in tube 1 and subsequently cooled under liquid nitrogen. The sample in tube 1, held by the apparatus, was heated by boiling water to vaporize the encapsulated solution. Tube 2 served as a cold trap to recover the solution that was driven out of the membrane sample. About 10–15 min were required to boil off the solution from the sample and recover it as condensed liquid. The composition of the condensed liquid was determined by means of gas chromatography (Varian type, Model 3400). The column (0.2% carbowax 1500 on

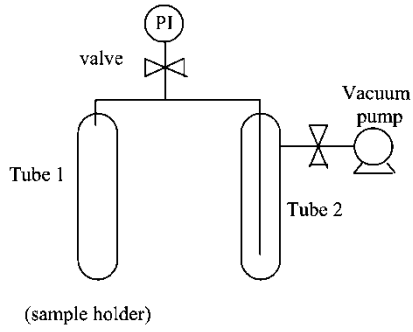

Figure 1. Schematic diagram of the apparatus used to determine the mixed liquid composition inside the polymeric membrane.

Downloaded At: 09:58 25 January 2011

80/100 carbopack C 6 ft. stainless steel) was operated isothermally at 170°C, with an inlet temperature of 200°C and a TCD detector temperature of 250°C.

The volume fraction, ϕ_i, in the ternary phase, was calculated from the product (u_i m) of the swelling ratio, m, and the relative volume fraction of a species in the membrane, u_i. At equilibrium, swelling ratio was taken to be equal to the sum of the volume fractions of species ($\phi_1 + \phi_2$).

Pervaporation Tests

Figure 2 shows the schematic diagram of the pervaporation experimental set up. The feed solution was loaded into a holding vessel (2.35 L), which was

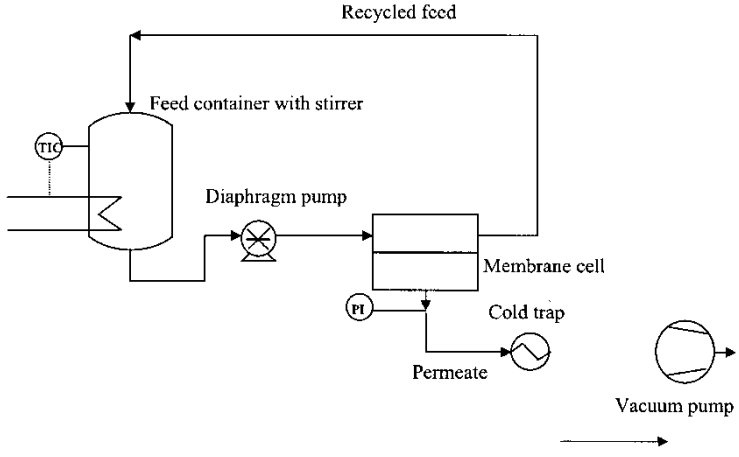

Figure 2. Schematic diagram of the pervaporation apparatus.

positioned at an elevated height and constant temperature. The solution gravitated down from the feed container to the pump and then was transferred to the permeation cell, which consisted of two compartments separated by a membrane. The retentate was returned to the feed container while the permeated vapor was collected in a cold trap. The feed variables were pressure, composition, temperature, and feed rate. A vacuum pump was used to keep the permeate-side pressure below the saturated vapor pressure of the permeating vapor (0.65 kPa). The feed temperature to the apparatus was controlled and kept constant by heating a tape, which was wrapped around the unit. Table 1 summarizes the feed conditions to the evaporator. A diaphragm pump (Preci Mini-PP model $125 \cdot D \cdot 3064 \cdot HC$) was used to supply a constant flow rate of 150 mL/minute to the membrane. We used a rectangular cell that could hold a flat membrane with an effective area of $0.0198\ m^2$.

The mole fractions of water in the feed solution were chosen to represent the actual water concentration obtained during esterification. The maximum yield of water for butanol esterification was estimated as 0.36-mole fraction at 70°C (ASPEN-simulation). Therefore, experiments with a water concentration of 0.40- and 0.50-mole fraction were performed for modeling purposes. However, we also synthesized an esterification mixture as feed to the reactor. The equilibrium composition was obtained by reacting acetic acid with butanol (1 : 1 mole ratio) and allowing the mixture to stand for 1 week in a sealed vessel over Nafion pellets at room temperature. Composition of the equilibrium mixture was analyzed by gas chromatography.

Downloaded At: 09:58 25 January 2011

DISCUSSION OF RESULTS

Swelling and Sorption Data

Figure 3 illustrates the swelling ratio of the membrane as a function of water fraction in the binary feed solutions (BuAc-H_2O, BuOH-H_2O, and

Table 1. Summary of feed mixtures to the evaporator

Mixture	Temperature range (°C)	Feed composition (X_{H_2O})
Water-butyl acetate	30–90	0.1–0.5
Water-butanol	70	0.1–0.5
Water-acetic acid	70	0.1–0.5
Equilibrium mixture	70	–

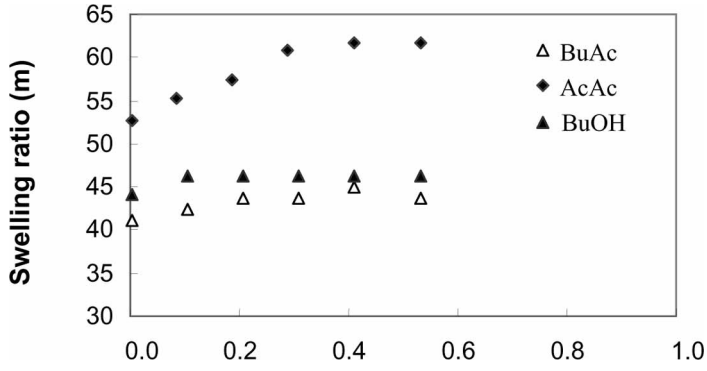

Figure 3. Effect of water-mole fraction in the feed on the swelling of the membrane at 70°C.

Downloaded At: 09:58 25 January 2011

AcAc-H_2O) at 70°C. The membrane exhibited swelling characteristics when contacted with aqueous solutions. The swelling ratio was highest for membrane samples that were contacted with the AcAc-H_2O mixtures ($X_{H_2}O = 0.55$-0.60), while the lowest swelling ratio was recorded for BuAc-H_2O solution ($X_{H_2}O = 0.45$-0.49). This result was attributed to differences in molecular size (acetic acid is smaller than butyl acetate), as well as ability of sorbed molecules to interact with the membrane matrix. We did not investigate the interaction behavior of an acid with the polymer matrix.

Figures 4, 5, and 6 compare the volume fractions of butanol, acetic acid, and butyl acetate absorbed by the membrane as a function of water-mole fraction. We found that addition of water molecules to butyl acetate, acetic acid, and butanol pure solutions significantly decreased their sorption capacity into the membrane. For example, above 0.4-mole fraction of water in the binary mixtures, BuOH-H_2O and BuAc-H_2O, the sorption of butanol and butyl acetate decreased significantly. This result confirms that water was preferentially sorbed by the membrane.

Permeation Data

In Figure 7, we compared the permeation of three binary mixtures at 70°C and $X_{H_2}O = 0.5$. The highest permeation of 4.2 kg/hour was recorded for BuAc-H_2O feed solution, while the lowest 0.75 kg/hour was observed for the AcAc-H_2O mixture. This result confirms that membrane flux depends on the amount of water that is preferentially sorbed by the membrane (Figs. 4, 5, and 6). At 70°C and 0.4-mole fraction of water in each binary

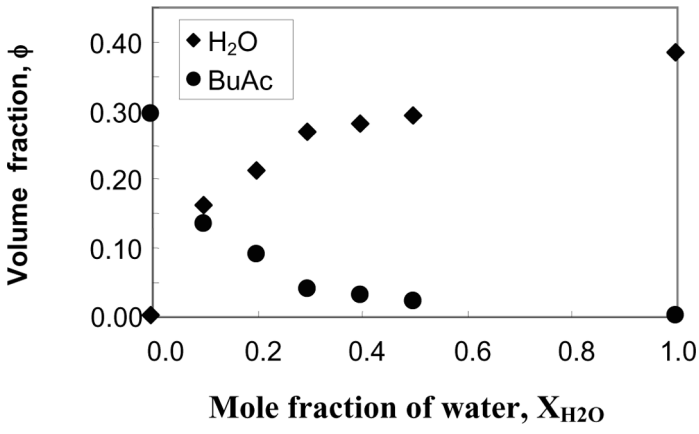

Figure 4. Volume fraction of butyl acetate in the membrane as a function of water-mole fraction in the binary feed at 70°C.

Downloaded At: 09:58 25 January 2011

feed, the fluxes of BuAc/H_2O, BuOH/H_2O, and AcAc/H_2O were 0.8, 0.4, and 0.25 kg/m^2 hour, respectively. Several researchers observed a similar trend for binary mixtures of ethanol-water and ethylene glycol-water (17).

The permeation flux was found to be strongly dependent on the feed solution temperature. Since the effect of temperature on the saturated vapor pressure of components is significant, we normalized the pervaporation flux by taking into account the transmembrane partial pressure difference. The Arrhenius-type of plot between flux and temperature was made and the

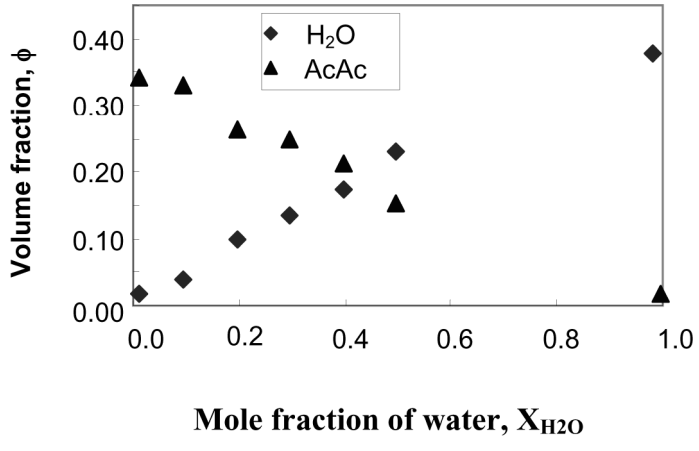

Figure 5. Volume fraction of acetic acid in the membrane as a function of water-mole fraction in the feed at 70°C.

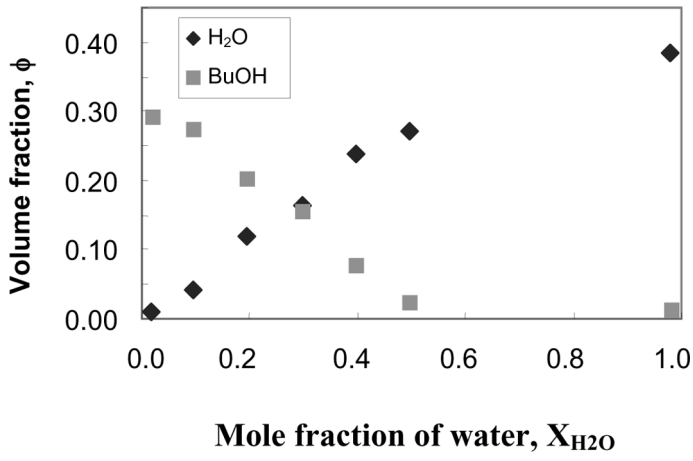

Figure 6. Volume fraction of butanol in the membrane as a function of water-mole fraction in the binary feed at 70°C.

Downloaded At: 09:58 25 January 2011

activation energies of transportation (Ep) were evaluated. Table 2 shows the activation energies for the mass transport of butyl acetate-water mixture at various water composition. The activation energy for the transport of water (14 kJ/mol) is much lower than that of butyl acetate (36 kJ/mol) at $XH_2O = 0.1$. This activation energy for water permeation was lower than that published in the literature for similar membranes (17). A plausible explanation for the low $E_{p,w}$ would be that an increase in swelling enhances the free rotation of the polymer segments about their chain axis, which reduces the energy barrier for water diffusion.

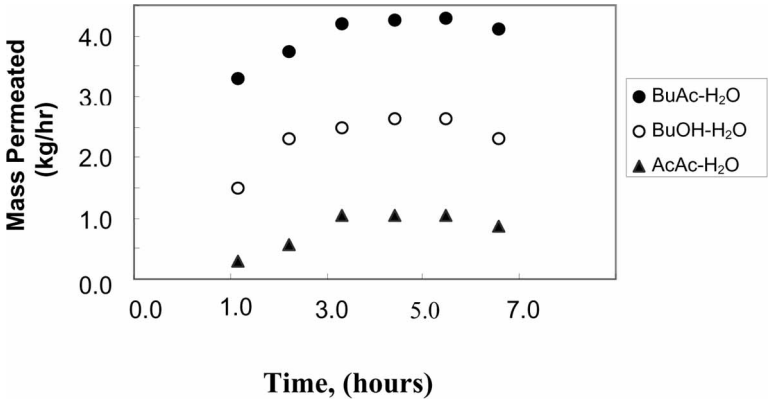

Figure 7. Mass permeation profiles of BuAc-H_2O, BuOH-H_2O, and AcAc-H_2O binary mixture at $X_{H_2}O = 0.5$ and 70°C.

Table 2. Activation energies (E_p) of permeation for the BuAc-H_2O mixture

Water in feed (X_{H_2O})	$E^*_{p,Tot}$ (kJ/mole)	$E^*_{p,W}$ (kJ/mole)	$E^*_{p,BuAc}$ (kJ/mole)
0.1	14	14	36
0.2	24	23	29
0.3	38	38	39
0.4	26	26	34
0.5	27	25	47

Figure 8 shows the total and partial fluxes of the components from the esterification mixture as a function of time. The initial esterification mixture had the following composition: $X_{BuOH} = 0.16$, $X_{AcAc} = 0.17$, $X_{H_2O} = 0.35$ and $X_{BuAc} = 0.32$ (i.e., 65% conversion) and was used as feed solution. Steady-state permeation was reached after 4 h for all the components. A higher conversion (95%) was achieved after using pervaporation.

An attempt was made to compare the effectiveness of pervaporation and distillation as separation techniques for binary mixtures. The VLE data of binary mixtures were calculated with ASPEN Tech V10 using the UNIQUAC activity coefficient model and the thermodynamic database of BuAc-H_2O mixture. By comparison, the pervaporation process yielded better separation data than that of distillation. The azeotropic point of the butylacetate-water mixture did not influence the separation since the mole fraction of water in the feed mixture was too low to form an azeotrope with butyl acetate (Fig. 9).

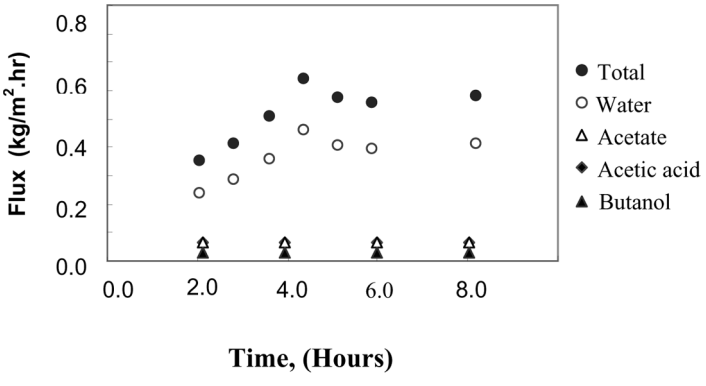

Figure 8. Flux profiles of individual components when the esterification mixture was fed to the membrane reactor at 70°C.

Downloaded At: 09:58 25 January 2011

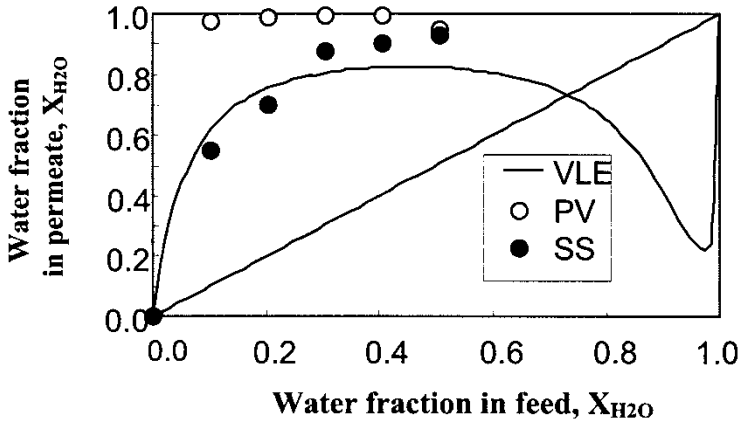

Figure 9. Comparison of pervaporation data (PV), sorption data (SS), and vapor–liquid equilibrium (VLE) data for the butyl acetate-water mixture, 70°C.

Downloaded At: 09:58 25 January 2011

Modeling of Sorption and Permeation Flux

Calculations for the preferential sorption were conducted with experimental values for the water-butyl acetate system at 30°C and 70°C since for esterification reactions the resultant solution is rich in butyl acetate and water. The concentration independent (constant) interaction parameters, χ_{13} and χ_{23}, were calculated from the swelling measurements by using Eq. (17). At a feed temperature of 70°C, $\phi_{3,w} = 0.62$ and $\phi_{3,BuAc} = 0.71$ from which it follows that χ_{13} and χ_{23} are 0.90 and 1.05, respectively.

Concentration-dependent interaction parameters were calculated by Eqs. (18) and (19), which carried some assumed literature values for the constants a, b, c, and d. Then, the Eqs. (18) and (19) were substituted into Eq. (14) to calculate the preferential sorption. We regressed the values of the interaction parameters using a Microsoft Excel 97 spreadsheet such that the least-squares error between the experimental and theoretical values for the preferential sorption reached the minimum. Table 3 shows the optimum interaction constants that were obtained for the penetrants. The molecular interpretation or the physical significance of the constant parameters a, b, c, and d is not available in the literature, but the parameters are widely applied to improve the agreement between theoretical and experimental data.

The values of the parameter g_{12} were calculated from Eq. (20) at the given volume fractions of water and butyl acetate, v_i, with known values of activities. The dependence of g_{12} on v_2 was expressed as a relation by plotting g_{12} against v_2 and then fitting a curve through the data with Microsoft Excel 97. A fourth-order polynomial was used as the base

Table 3. Activation energies (E_p) of permeation for the BuAc-H_2O mixture

Water in feed (X_{H_2O})	$E^*_{p,Tot}$ (kJ/mole)	$E^*_{p,W}$ (kJ/mole)	$E^*_{p,BuAc}$ (kJ/mole)
0.1	14	14	36
0.2	24	23	29
0.3	38	38	39
0.4	26	26	34
0.5	27	25	47

equation and a very good fit was achieved ($R^2 = 0.9981$). When concentration-dependent interaction parameters were used together with Eq. (14), the sorption process of butyl acetate-water mixture was described fairly accurately at feed temperatures 30°C and 70°C. This result is shown in Figs. 10 and 11. The simulated curves (solid lines) were calculated by using concentration-dependent interaction parameters. The ratio of predicted and measured values of sorption did not exceed 1.3, while the average deviation was about 10% for all the three binary mixtures.

With regard to modeling permeation flux, we assumed relevant values from published literature for the parameters $D_{0,i}$, $E_{D,i}$, κ_{ij}, and λ_{ij}. Then we used experimental values of ϕ_i to calculate theoretical values for the flux

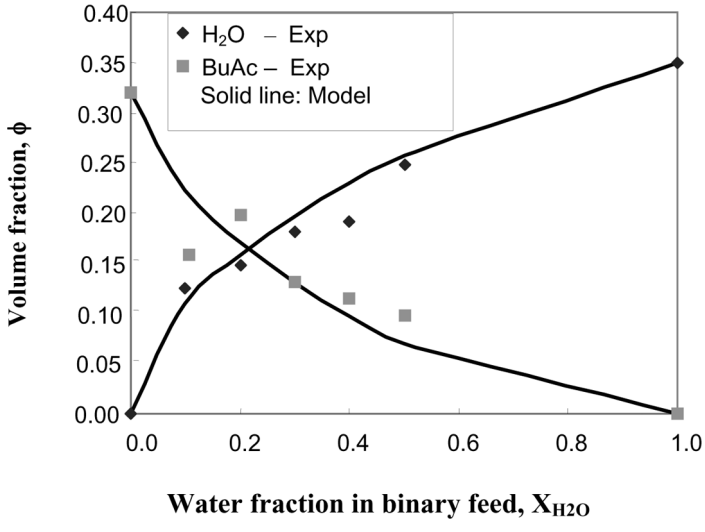

Figure 10. Modeling of sorption. The comparison of calculated and experimental sorption data at 30°C.

Downloaded At: 09:58 25 January 2011

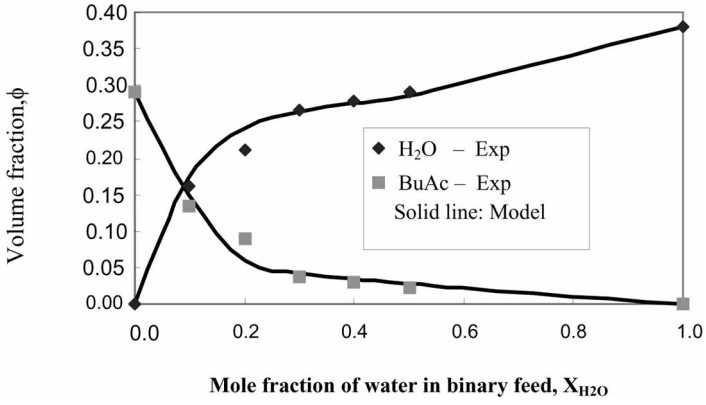

Figure 11. Modeling of sorption. The comparison of calculated and experimental solubility data of BuAc-H_2O feed at 70°C.

Downloaded At: 09:58 25 January 2011

using Eq. (24). Subsequently, we regressed the values of the parameters using a Microsoft Excel 97 spreadsheet such that the least-squares error between the experimental and theoretical values for the flux were at a minimum. The diffusion coefficients and activation energy of diffusion values were derived and are shown in Table 4.

It is difficult to compare the calculated diffusion coefficients at infinite dilution, $D_{0,i}$, with published data, because each system (chemicals and membranes) has its own unique transport characteristics. Yeom and Huang (18) modeled the permeation of ethanol-water mixtures by applying cross-linked PVA membranes. The values for $D_{0,W}$ that they found varied in the range $6.7 \times 10^{-9}\,m^2/hour$ (at 30°C)–$1.0 \times 10^{-8}\,m^2/hour$ (at 60°C) and for $D_{0,EtOH}$ in the range $1.1 \times 10^{-10}\,m^2/hour$ (at 30°C) to $2.6 \times 10^{-10}\,m^2/hour$ (at 60°C). Bagnell et al. (19) reported that the apparent diffusion coefficient for water was in the order of $1.1 \times 10^{-7}\,m^2/hour$ and for butanol in the order of $3.2 \times 10^{-8}\,m^2/hour$ at 30°C after using Nafion membranes. Our calculated values show fairly good comparison with the literature values.

In Table 5, it is clear that water exhibited the lowest activation energy of diffusion, E_D, while the E_D-value for butyl acetate was the highest. This is

Table 4. Concentration-dependent interaction parameter constants

Feed system	a	b	c	d
Water-butylacetate	0.3	−0.2	9.1	0.9
Water-butanol	0.8	−0.1	1.0	1.1
Water-acetic acid	0.8	2.4	0.2	−1.1

Table 5. Calculated values of apparent diffusion coefficients and activated energy of diffusion ($D_{0,i}$ and $E_{D,i}$)

	$D_{0,i}$ (m^2/h)	$E_{D,i}$ (kJ/mole)
Water	$3.8 \cdot 10^{-7}$	14
Butyl acetate	$6.7 \cdot 10^{-8}$	30
Butanol	$2.2 \cdot 10^{-9}$	20
Acetic acid	$3.1 \cdot 10^{-9}$	22

within reasonable expectation since the flux of water was the highest in all the experiments, while the butyl acetate flux was the lowest.

We proceeded to model the pervaporation of butyl acetate-water mixture. The calculated values of flux using the solution-diffusion model compared well the experimental flux values for butyl acetate-water feed. Figures 12 and 13 show the simulated and experimental fluxes of butyl acetate-water mixture at 30°C and 50°C. At both temperatures, the simulated and calculated values compared well within acceptable errors.

Downloaded At: 09:58 25 January 2011

CONCLUSIONS

Pervaporation of water from the esterification mixture was successfully carried out, resulting in enhanced conversion of reactants. Activated energy of diffusion for water molecules in the polymeric membrance was 14 kJ/mol, which was significantly lower than that of organic sorbents. The solution-diffusion model best described permeation flux.

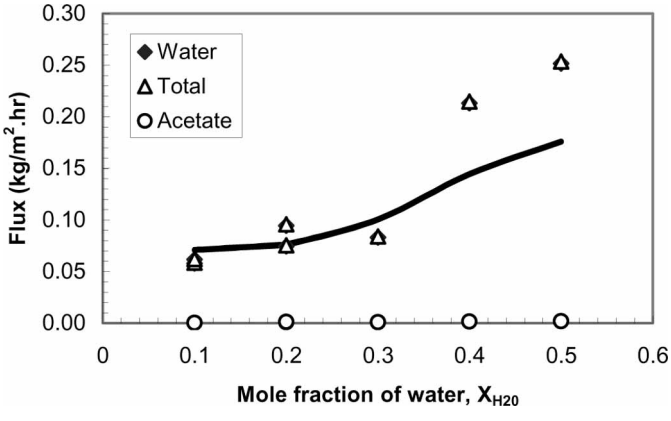

Figure 12. Modeling of BuAc-H_2O permeation flux. Comparison of calculated and experimental flux at 30°C.

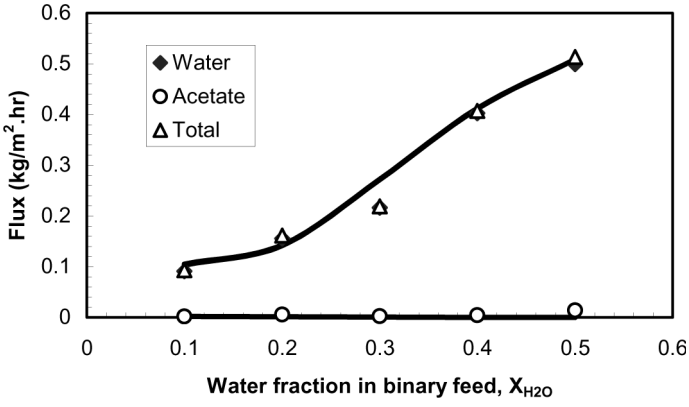

Figure 13. Modeling of BuAc-H_2O permeation flux. Comparison of calculated and experimental flux at 50°C. Solid line: model.

Downloaded At: 09:58 25 January 2011

LIST OF SYMBOLS

κ_{ij}	constant (−)
λ_{ij}	constant (−)
ρ_i	density ($kg \cdot m^{-3}$)
χ_{ij}	concentration independent binary interaction parameter (−)
ϕ_i	volume fraction in the ternary (membrane) phase (−)
μ_i	chemical potential of component i ($J \cdot mol^{-3}$)
Π	osmotic pressure (Pa)
a_i	activity ($mol \cdot m^{-3}$)
B_i	mobility in the membrane ($m^2 \cdot s^{-1}$)
C_i	concentration ($kg \cdot m^{-3}$)
d	constant
D_i	diffusion coefficient ($m^2 \cdot s^{-1}$)
D_{ij}	binary mass diffusion coefficient ($m^2 \cdot s^{-1}$)
E_D	activation energy of diffusion ($J \cdot mol^{-3}$)
g_{ij}	concentration dependent binary interaction parameter (−)
ΔG	free energy change ($J \cdot mol^{-3}$)
ΔG_{el}	elastic free energy ($J \cdot mol^{-3}$)
ΔG_M	Gibbs free energy of mixing ($J \cdot mol^{-3}$)
ΔH_M	Enthalpy change on mixing ($J \cdot mol^{-3}$)
L	membrane thickness (m)
I	distance (thickness of membrane) (m)
m	swelling ration (−)
n_i	mole fraction in ternary (membrane) phase (−)
R	universal gas constant ($J \cdot mol^{-1} \cdot K^{-1}$)

t	time (s)
ΔS_M	Entropy change on mixing ($J \cdot mol^{-1} \cdot K^{-1}$)
T	Temperature (K)
u_i	relative volume fraction in the membrane phase (−)
V	volume of swollen polymer (−)
V_i	molar volume ($m^3\,mol^{-1}$)
v_i	concentration (volume fraction) in feed (−)
W_o	initial mass of polymer (kg)
W_t	mass of polymer sample after lapse of time t (kg)
AA	acetic acid
BuAC	butyl acetate
BuOH	butanol

REFERENCES

Downloaded At: 09:58 25 January 2011

1. Aminabhavi, T.M., Harlapur, S.F., Balundgi, R.H., and Ortego, J.D. (1998) Theoretical and Experimental Investigations of Molecular Migration and Diffusion Kinetics of Organic Esters into Tetrafluoroethylene/propulene Copolymer Membranes. *Can. J. Chem. Eng.*, 76: 104–112.
2. David, M.-O., Gref, R., Nguyen, T.Q., and Neel, J. (1991a) Pervaporation-Esterification Coupling. I. Basic Kinetic Model. *Trans. Inst. Chem. Eng.*, 69: 335–340.
3. Zhu, Y. and Chen, H. (1998) Pervaporation Separation and Pervaporation-Esterification Coupling Using Crosslinked PVA Composite Catalytic Membranes on Porous Ceramic Plate. *J. Membr. Sci.*, 138: 123–134.
4. Cao, S., Shi, Y., and Chen, G. (1999) Pervaporation Separation of MeOH/MTBE Through CRA Membrane. *J. Appl. Polym. Sci.*, 71: 377–386.
5. Zhang, S. and Drioli, E. (1995) Pervaporation Membranes. *Sep. Sci. Technol.*, 30 (1): 1–3.
6. Huang, R.Y.M. and Shieh, J.-J. (1997) Pervaporation Separation of Ethanol-Water Mixtures Using Crosslinked Blend Membranes. *Sep. Sci. Technol.*, 32 (17): 2765–2784.
7. Flory, P. (1953) *Principles of Polymer Chemistry*, 1st Ed.; Cornell University Press: Ithaca, New York.
8. Heintz, A., Fuke, H., and Lightenthaler, R.N. (1991) Sorption and Diffusion in Pervaporation Membranes. In *Pervaporation Membrane Separation Processes*; Huang, R.Y.M., Ed.; Elsevier Publishers B.V.: Amsterdam, The Netherlands, Chapt.10.
9. Rhim, J.-W. and Huang, R.Y.M. (1989) On the Prediction of Separation Factor and Permeability in the Separation of Binary Mixtures by Pervaporation. *J. Membr. Sci.*, 46: 335–348.
10. Mulder, M.H.V., Franken, T., and Smolders, S.A. (1985) Preferential Sorption Versus Preferential Permeability in Pervaporation. *J. Membr. Sci.*, 22: 155–173.
11. Mulder, M.H.V. and Smolders, C.A. (1984) On the Mechanism of Separation of Ethanol/Water Mixtures by Pervaporation. I. Calculations of Concentration Profiles. *J. Membr. Sci.*, 17: 289–307.

12. Yang, J.S., Kim, H.J., Jo, W.H., and Kang, Y.S. (1998) Analysis of Pervaporation of Methanol-MTBE Mixtures Through Cellulose Acetate and Cellulose Triacetate Membranes. *Polymer.*, 39: 1381–1385.
13. Feng, X. and Huang, R.Y.M. (1997) Liquid Separation by Membrane Pervaporation: A Review. *Ind. Eng. Chem. Res.*, 36: 1048–1066.
14. Yoshikawa, M., Kuno, S.-I., and Kitao, T. (1994) Speciality Polymeric Membranes 3. Pervaporation Separation of Acetic Acid/Water Mixtures Through Polymeric Membranes Having a Pyridine Moiety as a Side Group. *J. Appl. Polym. Sci.*, 51: 1021–1027.
15. Chen, F.R. and Chen, H.F. (1998) A Diffusion Model of the Pervaporation Separation of Ethylene Glycol-Water Mixtures Through Crosslinked Poly(Vinyl Alcohol) Membrane. *J. Membr. Sci.*, 139: 201–209.
16. Huang, R.Y.M. and Yeom, C.K. (1991) Development of Crosslinked Poly(Vinyl Alcohol) (Type II) and Permeation of Acetic Acid-Water Mixtures. *J. Membr. Sci.*, 62 (1): 59–73.
17. Huang, R.Y.M. and Jarvis, N.R. (1970) Separation of Liquid Mixtures by Using Polymer Membranes. II. Permeation of Aqueous Alcohol Solutions Through Cellophane and Poly (Vinyl Alcohol). *J. Appl. Polym. Sci.*, 14: 2341–2356.
18. Huang, R.Y.M. and Yeom, C.K. (1990) Pervaporation Separation of Aqueous Mixtures Using Crosslinked Poly(Vinyl Alcohol). 2. Permeation of Ethanol-Water Mixtures. *J. Membr. Sci.*, 51 (3): 273–292.
19. Bagnell, L., Cavell, K., Hodges, A.M., Mau, A.W.-H., and Seen, A.J. (1993) The Use of Catalytically Active Pervaporation Membranes in Esterification Reactions to Simultaneously Increase Product Yield, Membrane Permselectivity and Flux. *J. Membr. Sci.*, 85: 291–299.

Downloaded At: 09:58 25 January 2011